Surface Science 641 (2015) 326–329

Contents lists available at ScienceDirect

Surface Science

journal homepage: www.elsevier.com/locate/susc

Primary excitation spectra in XPS and AES of Cu, CuO: Relative importance of surface and core hole effects

N. Pauly [a,*], S. Tougaard [b]

[a] Université Libre de Bruxelles, Service de Métrologie Nucléaire (CP 165/84), 50 av. F. D. Roosevelt, B-1050 Brussels, Belgium
[b] Department of Physics, Chemistry and Pharmacy, University of Southern Denmark, DK-5230 Odense M, Denmark

ARTICLE INFO

Available online 28 February 2015

Keywords:
XPS
AES
Core hole effect
Surface effect
Copper
Copper oxide

ABSTRACT

Quantitative interpretation of structures observed in XPS and AES requires models to correct for various physical processes involved. Besides the initial excitation process in XPS and AES, the measured spectrum is affected by three additional effects: the corehole(s), transport to the surface region and passage through the surface and vacuum regions. These three effects can be calculated by the QUEELS-XPS software (Quantitative analysis of Electron Energy Losses at Surfaces) in terms of energy-differential inelastic electron scattering cross sections. From this and the QUASES software (Quantitative Analysis of Surfaces by Electron Spectroscopy), background contributions and primary excitation spectra are obtained for various transitions (Cu 2p from Cu or CuO and Cu $L_3M_{23}M_{23}$) and we investigate the separate effect of bulk, surface, and core hole(s) excitations. We show that the shape of the XPS and AES primary spectra and background contributions are modified slightly by surface effects and very strongly by core hole(s) effects. For metals, the intrinsic excitations give rise to a prominent spike in the background close to the XPS-peak energy. This spike will be much reduced for wide band gap insulators. Moreover our method gives an easy procedure to obtain the true primary excitation spectra for XPS and AES.

1. Introduction

Accurate quantitative chemical analysis of solid surfaces by electron spectroscopies as X-ray photoelectron spectroscopy (XPS) or Auger electron Spectroscopy (AES) requires a correct understanding of several mechanisms. Indeed characteristic peaks are superimposed on a high background intensity of inelastically scattered electrons. Energy loss processes responsible for this background have two possible origins, namely intrinsic and extrinsic excitations [1–3]. Intrinsic excitations are caused by the electric field due to the sudden appearance of the static corehole(s) created during the excitation process. This field excites valence electrons and thus results in an energy loss by the emitted electron. Extrinsic excitations take place during the electron transport both inside the medium and in the vacuum and are due to the time and space varying electric field from the moving electron which also causes excitations and thereby energy losses. Extrinsic excitations are separated into bulk (occurring in the medium considered as infinite) and surface processes (occurring while the electron is moving in a shallow region in the medium and in the vacuum). The evaluation of the relative effect on the total background of each of these energy loss contributions is an important problem for accurate models of XPS or AES [4–8]. Indeed, surface and core hole effects blur attempts to rigorously compare experimental and pure theoretical results for XPS [9–11] and Auger [12,13] transition probabilities.

Recently two software, based on the semi-classical dielectric response theory, have been implemented to calculate the effective energy-differential inelastic electron scattering cross sections for reflection-electron-energy-loss spectroscopy (REELS) and also for XPS/AES, namely the QUEELS-ε(k,ω)-REELS software (QUantitative analysis of Electron Energy Losses at Surfaces) [14] and the QUEELS-XPS software (QUantitative analysis of Electron Energy Losses at Surfaces for XPS) [15], respectively. Comparison between cross sections obtained with these software and also with the cross section calculated for an infinite medium allows thus evaluation of the importance of each process.

An XPS/AES spectrum can be seen as the addition of the contributions from electrons that have undergone an increasing number of energy loss processes [16] and can thus be reproduced by the multiple convolution of a primary excitation function, $F(E)$, considered as an input parameter, with the energy-differential inelastic electron scattering cross section. It is however also possible to obtain $F(E)$ by deconvoluting the total spectrum with the inelastic cross section. It is precisely the goal of this paper to study the influence of the choice of the cross section (including or not surface and intrinsic effects) on the resulting primary excitation function. We emphasize that the objective of the present paper is to determine the effects of surface and core hole excitations on the XPS and AES excitation spectra. The resulting primary excitation spectra will facilitate comparison with theoretical

* Corresponding author. Tel.: +32 2 6502083; fax: +32 2 6504534.
E-mail address: nipauly@ulb.ac.be (N. Pauly).

http://dx.doi.org/10.1016/j.susc.2015.02.009
0039-6028/

calculations of the fundamental excitation mechanisms in XPS and AES. We thus do not intend with the present paper to study the usefulness of the cross sections K_{sc}^{XPS} for the usual procedures in quantitative XPS depth profiling which is based on analysis of the inelastic background.

In the following sections, we describe the model used in the QUEELS-ε(k,ω)-REELS software and QUEELS-XPS software as well as the procedure followed to obtain the primary excitation spectra of the chosen transitions (Cu 2p in Cu and CuO, Cu $L_3M_{23}M_{23}$). Results of $F(E)$ obtained by this method will then be discussed as a function of the considered inelastic cross section.

2. Scattering cross sections

The formalism implemented in both software (fully described in Ref. [17] and in Ref. [2] for REELS and XPS/AES, respectively) is based on the use of the surface reflection model describing the interactions of electrons with semi-infinite media in terms of the dielectric properties of the bulk material and incorporates the effects of the surface, of the static core hole(s) created during the ionization process (0 for REELS, 1 for XPS and 2 for AES), and excitations which occur as the electron travels in the vacuum, as well as interference between these effects. This allows determining three cross sections: first, $K_{sc}^{REELS}(E, \hbar\omega, \theta_i, \theta_o)$ the effective differential inelastic electron scattering cross section spectrum in REELS for an electron of energy E interacting with a solid and following a V-type trajectory making an angle θ_i (measured with respect to the surface normal) at the entrance and θ_o at the exit, second, $K_{sc}^{XPS}(E, \hbar\omega, \theta)$, the effective differential inelastic electron scattering cross section spectrum in XPS for a photoelectron of energy E following a straight line trajectory inside the solid with the angle θ measured with respect to the surface normal, and third, $K_{sc}^{AES}(E, \hbar\omega, \theta)$ corresponding to the effective differential inelastic electron scattering cross section for an Auger electron.

To calculate K_{sc}^{REELS}, K_{sc}^{XPS} and K_{sc}^{AES} within this formalism, we use the QUEELS-ε(k,ω)-REELS and QUEELS-XPS software [14,15] (which allow considering 1 or 2 core holes) for which the only required input is the energy loss function (ELF) of the medium, Im $\{-1/\varepsilon(k,\omega)\}$. To evaluate it, we consider, as a model, the expansion in Drude–Lindhard type oscillators [18]:

$$\mathrm{Im}\left\{-\frac{1}{\varepsilon(k,\omega)}\right\}=\sum_{i=1}^{n}\frac{A_i\hbar\gamma_i\hbar\omega}{\left(\hbar^2\omega_{0ik}^2-\hbar^2\omega^2\right)^2+\hbar^2\gamma_i^2\hbar^2\omega^2}\theta(\hbar\omega-E_G) \quad (1)$$

with the dispersion relation:

$$\hbar\omega_{0ik}=\hbar\omega_{0i}+\alpha_i\frac{\hbar^2k^2}{2m}. \quad (2)$$

A_i, $\hbar\gamma_i$, $\hbar\omega_{0ik}$ and α_i are the strength, width, energy and dispersion of the ith oscillator, respectively and the step function $\theta(\hbar\omega - E_G)$ is included to describe the effect of the energy band gap E_G present in semiconductors and insulators. The parameters in the expansion are taken from Ref. [19] for the materials studied in this work, namely, Cu and CuO.

For the calculation of the inelastic cross section of an electron travelling in an infinite medium (and for which only bulk interactions must be consequently considered), K_{bulk}, we have used the same Drude–Lindhard expansion of the ELF. Moreover we note that, for REELS, the electron crosses the surface twice which prevents the direct use of K_{sc}^{REELS} to describe an XPS configuration. We have therefore adjusted K_{sc}^{REELS} to obtain $K_{b+s} = 0.5 \times (K_{sc}^{REELS} + K_{bulk})$ which corresponds to an electron travelling in the medium and crossing the surface once. This calculation is correct if we neglect the coupling effects between the incoming and outgoing trajectories in the V-type trajectory of REELS [20].

Fig. 1 shows the inelastic scattering cross sections K_{sc}^{XPS} obtained for photoelectrons of 320 eV energy emitted at an angle $\theta = 15^o$ with respect to the surface normal from pure Cu and CuO samples which are two cases studied here (Cu $2p_{3/2}$ photoelectron excited by a Mg Kα X-ray source). We also show the inelastic scattering cross sections K_{sc}^{AES} corresponding to same conditions but with 2 static core holes, K_{bulk} calculated for an electron of 320 eV energy travelling in an infinite medium as well as K_{b+s} calculated from K_{bulk} and K_{sc}^{REELS} for $E = 320$ eV, $\theta_i = 15^o$ and $\theta_o = -15^o$ (and thus for quite different incoming and outgoing electron trajectories justifying the neglect of interference effect between them [20]). We note that, for Cu and CuO, $K_{sc}^{AES} > K_{sc}^{XPS} \gg K_{b+s} > K_{bulk}$ for energy loss <10 eV but similar for large energy losses. The major difference between Cu and CuO is the presence of the band gap for CuO which implies zero scattering cross sections for energy losses smaller than 1 eV.

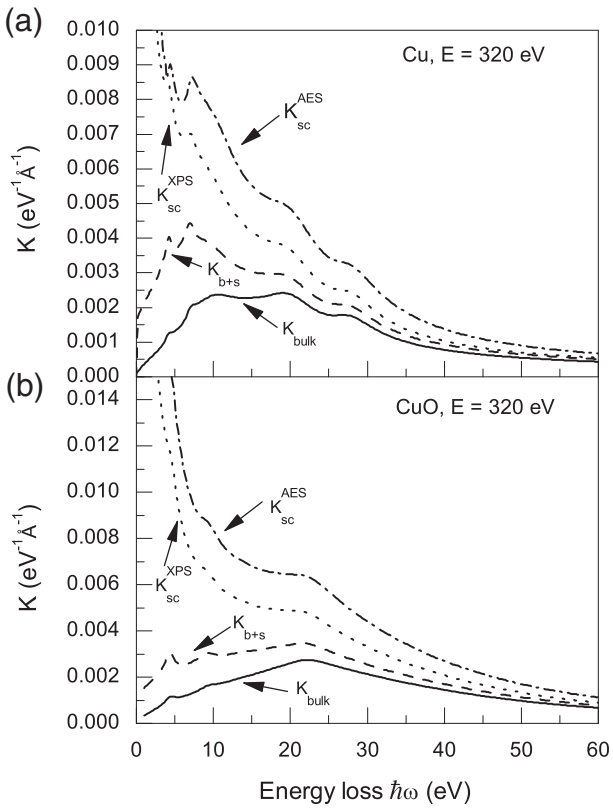

Fig. 1. Energy-differential inelastic electron scattering cross sections, for (a) Cu and (b) CuO, K_{sc}^{AES} (320, $\hbar\omega$, 15°) (dash-dotted line) K_{sc}^{XPS}(320, $\hbar\omega$, 15°) (dotted line), K_{b+s}(320, $\hbar\omega$, 15°) (dashed line), and K_{bulk}(320, $\hbar\omega$) (solid line).

3. Experiment

The experimental XPS spectra of pure Cu and CuO were excited with a non-monochromatic Mg Kα X-ray source, while the Auger spectrum of pure Cu was obtained with an Al Kα source. The spectra were recorded with a hemispherical analyzer at a constant pass energy of 20 eV and were corrected by the function $E^{-0.7}$ to take into account the energy dependence of the analyzer transmission. The X-ray incident and photo- and Auger electron exit angles were respectively 34° and 15° with respect to the surface normal. The ambient pressure was about 10^{-10} mbar. Complete experimental descriptions, including the procedure used to produce the CuO sample, can be found in Refs. [8,19].

The background subtraction using different scattering cross sections K_{sc}^{XPS}, K_{sc}^{AES}, K_{b+s} and K_{bulk} was accomplished with the QUASES software package [21] that thus allows obtaining the corresponding primary excitation spectrum including or not surface and/or intrinsic effects.

4. Results and discussion

Fig. 2 shows the results of the deconvolution procedure for Cu (primary spectrum and background) obtained with the K_{bulk}, K_{b+s} and K_{sc}^{XPS} cross sections. It is clear that the background, and consequently the $F(E)$ function, is strongly influenced by the choice of the cross section. Comparing the background corresponding to the use of K_{bulk} (Fig. 2(a)) and K_{b+s} (Fig. 2(b)), we observe that surface excitations cause the background intensity to be slightly larger in the 0–10 eV energy loss range. However, much larger differences are seen (in Fig. 2(c)) as the result of intrinsic excitations which even give rise to a prominent spike in the background at zero energy loss due to the large value of the scattering cross section for small energy losses (see Fig. 1). Moreover, when K_{sc}^{XPS} is used (Fig. 2(c)), including thus bulk, surface and intrinsic energy loss processes, the resulting $F(E)$ is the true primary excitation spectrum which accounts for all effects that are part of the initial photo-excitation process like life time broadening, spin–orbit coupling and multiplet splitting (we note also in this spectrum the contributions from the K_{α_3} and K_{α_4} lines). Indeed, this $F(E)$ spectrum agrees well, as shown in Fig. 3, with the result obtained by the convolution procedure used in Ref. [7] and this was found to agree well with theoretical evaluations (see Ref. [7] for a full discussion). As shown in Ref. [7], in the resulting primary excitation spectra, for each of the 2p3/2 peaks corresponds a 2p1/2 peak with exactly half the intensity and at an energy exactly 20 eV smaller.

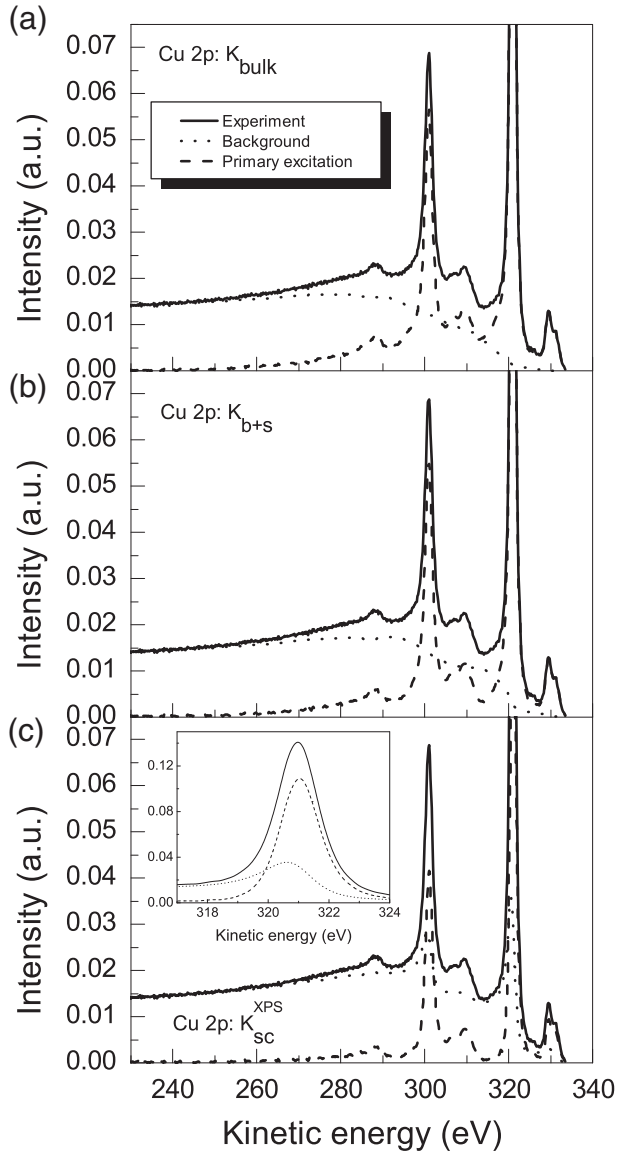

Fig. 2. Results of the background subtraction procedure using QUASES for the Cu 2p emission from pure Cu using (a) K_{bulk}, (b) K_{b+s} and (c) K_{sc}^{XPS}. For each case, experiment (solid line), background (dotted line) and $F(E)$ spectrum (dashed line) are shown. The inset in (c) shows an expansion of the Cu 2p3/2 peak.

Fig. 4 shows equivalent results of Cu 2p emission from a CuO target. $F(E)$ functions and backgrounds are now directly compared for each type of scattering cross section in Fig. 4(a) and (b), respectively. Similar to the results for Cu, we observe that compared to bulk excitations, surface excitations cause a small increase in the background intensity while the core hole (K_{sc}^{XPS}) results in a considerable increase. However, the spike in the background at small energy loss is much smaller for CuO because the ~1 eV band gap prevents intrinsic excitations with energy less than the band gap energy. In general, we thus expect that for metals, there is a prominent spike in the background close to the XPS-peak energy, the intensity of which is much reduced for insulators with a wide band gap.

Finally our procedure with QUASES can also be applied to Auger spectra. This is shown in Fig. 5 for the case of $L_3M_{23}M_{23}$ Auger transition from pure Cu. In this calculation we have considered K_{bulk}, K_{sc}^{XPS} and K_{sc}^{AES} cross sections in the deconvolution procedure; previous $F(E)$ function obtained by the fitting procedure in Ref. [8] is also shown. As for XPS, the true $F(E)$ function is obtained when the appropriate cross section is used, K_{sc}^{AES} in this case (as proved by the good agreement of this function with the result of Ref. [8]), while for other cross sections the background is underestimated. We observe that using the cross section K_{sc}^{AES} corresponding to two core holes results in a significant change compared to using K_{sc}^{XPS} which corresponds to one core hole.

5. Conclusion

In this work, we have studied a simple method to calculate the background corrected XPS and AES spectra taking into account the various intrinsic and extrinsic energy loss processes involved. Cross sections, including surface and core hole effects, were calculated with the QUEELS-XPS software and the background correction was done with the QUASES software using these cross sections.

The effective cross section for electron energy loss in Cu at 320 eV showed significant influence of surface excitations, and in particular a

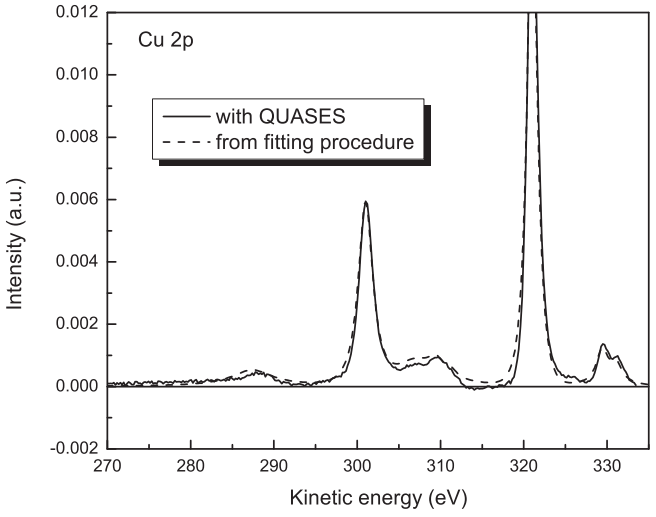

Fig. 3. Comparison of the primary excitation functions $F(E)$ for Cu 2p obtained in the present work (solid line) and with the fitting procedure in Ref. [7] (dashed line).

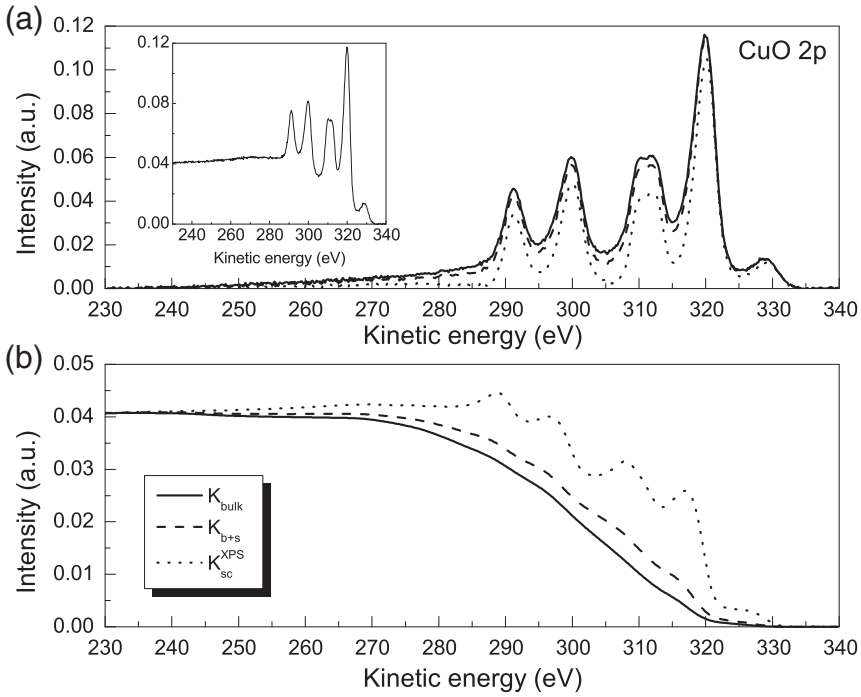

Fig. 4. Results of the background subtraction procedure using QUASES for CuO. (a) $F(E)$ functions calculated with K_{bulk} (solid line), K_{b+s} (dashed line) and K_{sc}^{XPS} (dotted line); (b) corresponding backgrounds. Experimental spectrum is shown in the inset of (a).

very large influence of intrinsic excitations due to one core hole (K_{sc}^{XPS} corresponding to the XPS case) and two core holes (K_{sc}^{AES} corresponding to the AES case). The cross sections for CuO show a similar trend with the important difference that intrinsic excitations are absent for energy loss less than ~1 eV corresponding to the band gap energy.

We have specifically compared separately the effect of bulk, surface, and core hole effects on Cu 2p spectra from pure Cu and CuO. We found that surface effects increase the background intensity slightly in the near peak energy loss region. In contrast, the effects of the core hole are huge and they even create a spike in the background within the main peak for very low energy loss. This spike is less pronounced for CuO due to the band gap which prevents intrinsic excitations with energy loss less than the band gap energy. In general, we expect that XPS from metals will have a prominent peak in the background close to the XPS-peak energy and that this is much reduced for insulators with a wide band gap.

For AES it is found that using K_{sc}^{XPS} underestimates the background intensity significantly compared to using K_{sc}^{AES} because the probability for excitations due to two core holes is considerably larger than for one core hole.

Moreover, we have shown that the true primary excitation spectrum, which includes all the effects which are part of the initial photoexcitation or Auger process, is obtained when the K_{sc}^{XPS} cross section is used for XPS and K_{sc}^{AES} for Auger. These $F(E)$ spectra can be compared with potential theoretical calculations and we hope this will lead to a better understanding of the fundamental mechanisms behind photo- and Auger emissions.

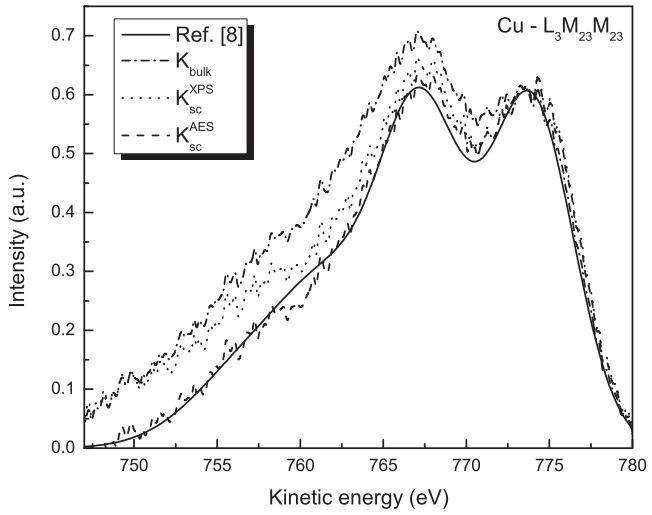

Fig. 5. $F(E)$ functions for $L_3M_{23}M_{23}$ Auger transition from pure Cu calculated with K_{bulk} (dash-dotted line), K_{sc}^{XPS} (dotted line) and K_{sc}^{AES} (dashed line); pure primary excitation function obtained by the fitting procedure in Ref. [8] is also shown (solid line).

References

[1] P.H. Citrin, G.K. Wertheim, Y. Baer, Phys. Rev. B 16 (1977) 4256.
[2] A.C. Simonsen, F. Yubero, S. Tougaard, Phys. Rev. B 56 (1997) 1612.
[3] S. Tougaard, J. Electron Spectrosc. Relat. Phenom. 178–179 (2010) 128.
[4] J. Vegh, Surf. Sci. 577 (2005) 220.
[5] F. Yubero, S. Tougaard, Phys. Rev. B 71 (2005) 045414.
[6] F. Yubero, S. Tougaard, J. Electron Spectrosc. Relat. Phenom. 185 (2012) 552.
[7] N. Pauly, S. Tougaard, F. Yubero, Surf. Sci. 620 (2014) 17.
[8] N. Pauly, S. Tougaard, F. Yubero, Surf. Sci. 630 (2014) 294.
[9] K. Okada, A. Kotani, J. Electron Spectrosc. Relat. Phenom. 52 (1990) 313.
[10] P.S. Bagus, E.S. Ilton, Phys. Rev. B 73 (2006) 155110.
[11] E. Stavitski, F.M.F. de Groot, Micron 41 (2010) 687.
[12] E. Antonides, E.C. Janse, G.A. Sawatzky, Phys. Rev. B 15 (1977) 1669.
[13] E. Antonides, E.C. Janse, G.A. Sawatzky, Phys. Rev. B 15 (1977) 4596.
[14] S. Tougaard, F. Yubero, QUEELS-$\epsilon(k,\omega)$-REELS: Software Package for Quantitative Analysis of Electron Energy Loss Spectra; Dielectric Function Determined by Reflection Electron Energy Loss Spectroscopy, Version 4.3 See http://www.quases.com/ 2014.
[15] S. Tougaard, F. Yubero, QUEELS-XPS: Quantitative Analysis of Electron Energy Loss in XPS Spectra, Version 2.1 See http://www.quases.com/2011.
[16] S. Tougaard, P. Sigmund, Phys. Rev. B 25 (1982) 4452.
[17] F. Yubero, J.M. Sanz, B. Ramskov, S. Tougaard, Phys. Rev. B 53 (1996) 9719.
[18] R.H. Ritchie, A. Howie, Philos. Mag. 36 (1977) 463.
[19] D. Tahir, S. Tougaard, J. Phys. Condens. Matter 24 (2012) 175002.
[20] N. Pauly, S. Tougaard, F. Yubero, Phys. Rev. B 73 (2006) 035402.
[21] S. Tougaard, QUASES, Ver. 5.1, 2005, Software Packages to Characterize Surface Nano-Structures by Analysis of Electron Spectra See http://www.quases.com/.